Earth Surface Processes and Landforms
Earth Surf. Process. Landforms **33**, 280–294 (2008)
Published online 13 July 2007 in Wiley InterScience
(www.interscience.wiley.com) **DOI:** 10.1002/esp.1545

Monitoring of the sediment dynamics along a sandy shoreline by means of airborne hyperspectral remote sensing and LIDAR: a case study in Belgium

B. Deronde,[1]* R. Houthuys,[1] J.-P. Henriet[2] and V. Van Lancker[2]
[1] *Remote Sensing and Earth Observation Processes (TAP), Flemish Institute for Technological Research (VITO), Mol, Belgium*
[2] *Renard Centre of Marine Geology, Universiteit Gent – Geology and Soil Science, Gent, Belgium*

**Correspondence to: Bart Deronde, Flemish Institute for Technological Research (VITO), Remote Sensing and Earth Observation Processes (TAP), Boeretang 200, 2400 Mol, Belgium.*
E-mail: Bart.deronde@vito.be

Received 13 February 2007;
Revised 28 April 2007;
Accepted 12 May 2007

Abstract

Airborne hyperspectral data and airborne laserscan or LIDAR data were applied to analyse the sediment transport and the beach morphodynamics along the Belgian shoreline. Between 2000 and 2004, four airborne acquisitions were performed with both types of sensor. The hyperspectral data were classified into seven sand type classes following a supervised classification approach, in which feature selection served to reduce the number of bands in the hyperspectral data. The seven classes allowed us to analyse the spatial dynamics of specific sediment volumes. The technique made it possible to distinguish the sand used for berm replenishment works or for beach nourishments from the sand naturally found on the backshore and the foreshore. Subtracting sequential DTMs (digital terrain models) resulted in height difference maps indicating the erosion and accretion zones. The combination of both data types, hyperspectral data and LIDAR data, provides a powerful tool, suited to analyse the dynamics of sandy shorelines. The technique was demonstrated on three sites along the Belgian shoreline: Koksijde, located on the West Coast and characterized by wide accretional beaches, influenced by dry berm replenishment works and the construction of groins; Zeebrugge, on the Middle Coast, where a beach nourishment was executed one year before the acquisitions started and where the dams of the harbour of Zeebrugge are responsible for the formation of a large accretional beach, and Knokke-Heist, located on the East Coast and characterized by narrow, locally reflective, beaches, heavily influenced by nourishment activities. The methodology applied allowed retrieval of the main sediment transport directions as well as the amount of sediment transported. It proved to be specifically suited to follow up the redistribution and the re-sorting of the fill in beach nourishment areas.

Keywords: airborne hyperspectral remote sensing; LIDAR; beach morphodynamics; sediment transport; sandy shoreline; Belgium

Introduction

This paper illustrates how the combination of two state-of-the-art remote sensing techniques can be used to study the sediment dynamics, and hence the morphodynamics, along sandy shorelines. The term morphodynamics was introduced into the coastal literature by Wright and Thom (1977). They defined it as the 'mutual adjustment of topography and fluid dynamics involving sediment transport'. On beaches, this implies that the surface topography of the beach will adjust to accommodate the fluid motions produced by the waves, tides and other currents, which in turn will influence the wave and tide processes. As we also studied the geomorphological changes on the backshore, i.e. the part of the beach between the high-water mark and the dune foot (Figure 1), aeolian forces should also be taken into account (Short, 2001; van der Wal, 1998, 2000a, 2000b). An exhaustive overview of the scientific literature concerning beach and shoreface morphodynamics can be found in the work of Short (2001).

Remote sensing in general is a very powerful tool for beach monitoring and investigation, since it allows collection of spatially continuous information over a vast area in a short time frame. The latter is highly important in coastal

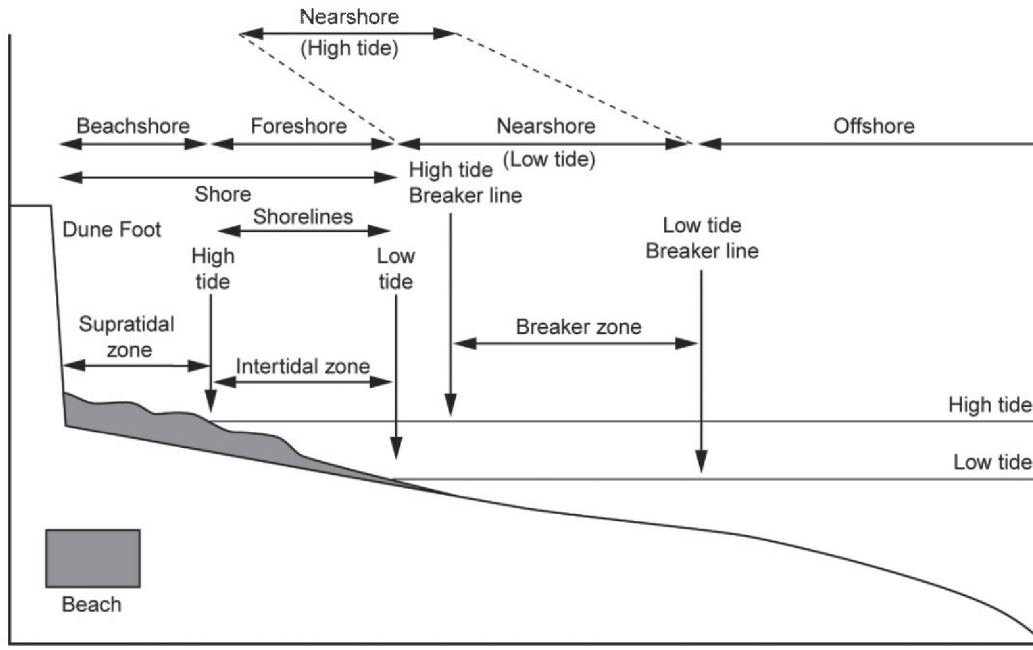

Figure 1. Coastal terminology (Bird, 2000).

areas as this environment is subject to fast changes in time. Moreover, the technique is not hampered by the (in)accessibility of a site, which is often a problem in coastal areas. However, the common spaceborne platforms, making use of sun-synchronous satellites, are limited by their fixed orbit. This implies that acquisitions cannot be planned in time; hence, tides and weather often prohibit successful acquisitions. Airborne remote sensing on the other hand, although often more expensive, is much more flexible. It allows a mission to be planned carefully, taking into account all possible constraints. Cracknell (1999) and subsequently Malthus and Mumby (2003) provided an overview of the capacities of remote sensing for estuarine and coastal zone studies. While the focus in these review articles is mainly on low-resolution remote sensing, Mumby and Edwards (2002) investigated the additional value of very high-resolution data (IKONOS) and hyperspectral data (CASI, see further).

The methodology adopted in this paper is based on two types of airborne remote sensing: airborne hyperspectral remote sensing and airborne laserscanning.

Hyperspectral remote sensing, or imaging spectroscopy, is the acquisition of images in tens to hundreds of (contiguous) spectral bands such that for each pixel element in an image a complete reflectance spectrum is available (Goetz, 1992). Reflectance is defined as the ratio of the radiance of the reflected light over the radiance of the incoming light at a certain wavelength. Each pixel element contains a unique reflectance spectrum that can be used for the identification of the Earth's surface materials. When light interacts with the Earth's surface, certain wavelengths are preferentially absorbed, whereas other wavelengths are transmitted or reflected. The kind of material determines the degree to which light of different wavelengths is absorbed. The part of the sunlight not absorbed (or transmitted) is reflected and determines the colour of the material. In this way, each material has its own spectral signature by which it can be identified.

A LIDAR (light detection and ranging) system is a scanner that deflects a laser beam across the flight line and detects its reflection, so that a swath of ground along the flight line is sampled pointwise. The distance to the Earth's surface is determined by measuring the pulse return time. The position and attitude of the sensor is calculated from d-GPS (differential-GPS) and INS (inertial navigation system) measurements. In combination with the scan angle, the 3D position of each laser beam spot on the surface can be determined. On flat unvegetated surfaces, a vertical accuracy of 5–10 cm can be achieved. The development of LIDAR represents a technological breakthrough in topographic monitoring. A number of studies have demonstrated the ability of LIDAR data to accurately represent topography over large sections of coastline (Revell *et al.*, 2002; Sallenger *et al.*, 2003; White and Wang, 2003), and sequential LIDAR surveys have shown that shoreline changes can be monitored over time (Stockdon *et al.*, 2002). Brock *et al.* (2002) provide a good overview of the basic principles of airborne laser altimetry.

DOI: 10.1002/esp

The methodology adopted in this paper is applied on the Belgian shoreline (see the 'Study Area' section) and covers the period between 2000 and 2004. To demonstrate the capabilities of the methodology, three study sites, each with a distinct beach morphology and dynamic behaviour, are elaborated. The 5 year time frame allows us to gain insight into the longer-term dynamics without focusing on yearly changes, which often do not point on a trend in the longer term and hence are not relevant for the erosion problematic in the longer term.

It should be noted that the first aim of coastal morphological monitoring in Belgium is to determine the safety level of the seawall and to manage the measures needed to keep the safety at this level. The coastal barrier indeed protects an up to 20 km wide strip of coastal lowland from flooding. For the low-lying countries, such as Belgium, efficient monitoring is a prerequisite in the view of an expected sea-level rise of 10–90 cm by 2100, depending on the model used (IPCC, 2001). In April 2007, at the Eighth Session of Working Group II of the Intergovernmental Panel on Climate Change (IPCC), held in Brussels (Belgium), the IPCC published its *Summary for Policymakers*, stating that 'Coasts are projected to be exposed to increasing risks, including coastal erosion, due to climate change and sea-level rise. The effect will be exacerbated by increasing human-induced pressures on coastal areas'.[1] This statement certainly holds for the Belgian shoreline. According to the same report, 'storminess' will increase, causing important economic losses for many coastal nations (Mills, 2005). The combination of higher sea levels with more extreme weather events necessitates a regular and detailed mapping of the shorelines under pressure, applying the most suited techniques. In addition, if data can be obtained on the state and the dynamics of the coastal sediment budget, it can be better estimated how well beach sections recover from erosive events and whether there is sufficient sediment available to cope with sea-level rise.

Study Area

The Belgian coast is situated at the southern edge of the North Sea basin (Figure 2). It has a length of 65 km from De Panne in the Southwest to Knokke-Heist in the Northeast. From a geological point of view, this coastline is part of the 'Flemish coastal plain', a depositional system at the southern edge of the North Sea Basin, which is commonly known

Figure 2. The Belgian coast is situated along the southern shores of the North Sea. It has a length of 65 km between the French border in the Southwest and the Dutch border in the Northeast.

[1] http://www.ipcc.ch/SPM13apr07.pdf

DOI: 10.1002/esp

as the Southern Bight (Rottier and Arnoldus, 1984). The actual coastline was shaped during the Holocene and is believed to have been formed by sand derived by the erosion of the Pleistocene basement and from the tide-induced cross-shore transport from the North Sea. Houthuys *et al.* (1993) give a good overview of the recent geological and historical evolution of the Belgian coastal plain (see also the work of Beets and Van Der Spek, 2000; Baeteman and Declercq, 2002).

The Belgian coast consists of a sandy beach barrier, which, at low tide, is up to 600 m wide in De Panne and Koksijde, both situated on the West Coast. These beaches are characterized by low-gradient surf zones, across which spilling breakers dissipate their energy. According to the beach state index (BSI) of McLachlan *et al.* (1993), which indicates the ability of waves and tides to move sand, these beaches can be classified as ultra-dissipative. This means that the tide range is large and the wave energy high. Figure 3(A) shows a profile of the beach in De Panne obtained

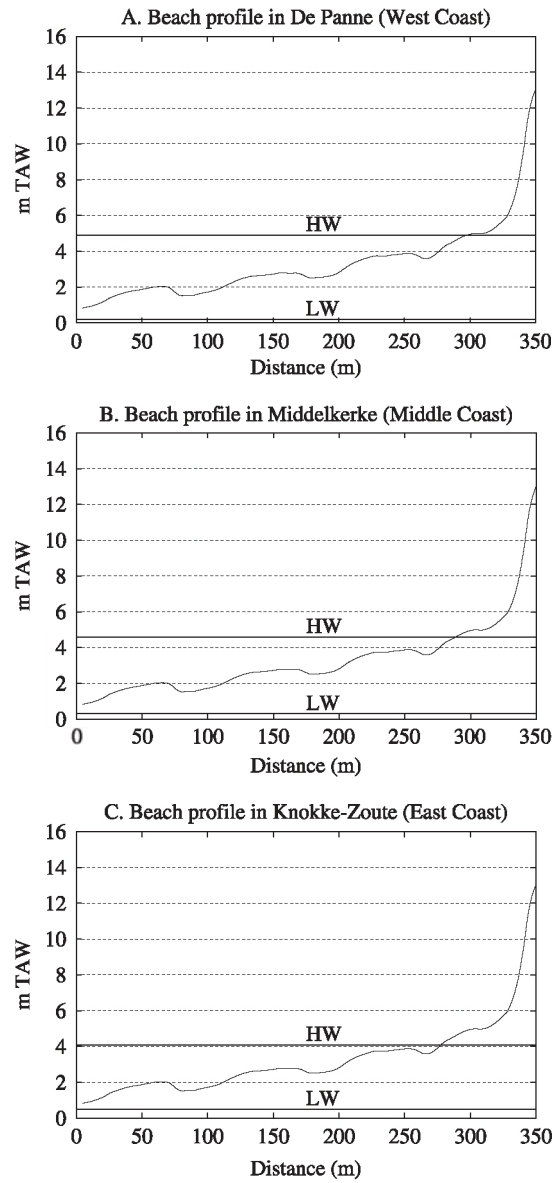

Figure 3. Beach profile at the Belgian West Coast, Middle Coast and East Coast. The data are derived from an airborne LIDAR survey in September 2004. The upper black line indicates the local mean high water level (HW); the lower black line indicates the local mean low water level (LW). TAW is the local reference level.

DOI: 10.1002/esp

with airborne laserscanning. Here, the intertidal part of the beach contains several parallel ridges and runnels which pass into the supratidal beach. The mean slope is between 1 and 1.5%. The beaches of the West Coast are the most natural beaches along the Belgian shoreline; they are not influenced by large-scale nourishment works although a few groins, beach groins and yearly dry berm replenishment works (or beach scrapings) influence the profile locally. The latter is especially the case in Koksijde.

The Middle Coast, i.e. the coastal strip between Middelkerke and Zeebrugge (Figure 2), is characterized by less wide beaches: on average between 200 and 400 m. Although they still qualify as ultra-dissipative beaches, their geomorphology is completely different from the geomorphology of the beaches along the West Coast. This is mainly due to the groins that have been placed along the entire Middle Coast, except for the coastal strip around De Haan. The resulting profile is rather smooth between the low- and high-water marks and has an average slope of 1.5–2.0%, while the backshore is much steeper (more than 5%). The beach has a concave profile around the high-water mark (Figure 3(B)). The Middle Coast has been the scene for large-scale nourishment works, especially around De Haan, where in the 1990s a classical dry beach nourishment was combined with the deposition of a nearshore feeder berm (De Wolf and Houthuys, 1997). Recently, in the spring of 2004, a beach nourishment took place in the centre of Oostende (also combined with the deposition of a nearshore berm). Before the nourishment there was no longer a dry beach in this location, which means that at high tide the sea dike immediately served as a seawall. Many places on the Middle Coast are also subject to dry berm replenishment works.

The East Coast and especially Knokke-Heist features the narrowest beaches in Belgium. They are only 100–300 m wide with a mean slope of 1.5–2.5% on the intertidal part. According to the beach state index, they are classified as dissipative, although local reflective conditions occur around the high-water mark. These beaches have for many decades been prone to heavy erosion. Therefore, man has striven to keep this shoreline at its position since the late 1970s, making use of large-scale dry beach nourishments in combination with groins. The effect of the beach nourishments on the dry beach is clearly visible in Figure 3(C) as a berm around the high-water level. It should also be noted that the median grain size is significantly coarser on the East Coast (250–400 μm) than on the Middle (170–250 μm) and the West Coast (150–200 μm). This is not only a natural gradient, but it is influenced and reinforced by the nourishment activities, driven by the knowledge that coarser sediments are less prone to erosion. More details about the sedimentological composition of the sand along the Belgian shoreline can be found in the work of Deronde *et al.* (2006a). More on the geomorphology and dynamics of the Belgian beach is found in the work of De Moor (2006).

The methodology explained in the next section was applied to the entire Belgian coastline. However, to avoid going too much into detail, we discuss in this paper the results for three specific sites: the wide beach of Koksijde, situated on the West Coast and close to the French border, the accretional beach of Zeebrugge, located west of the dams of the harbour of Zeebrugge, and the narrow erosive beach of Knokke-Heist, situated between the eastern dam of the harbour of Zeebrugge and the Dutch border. These very different and interesting sites allow us to demonstrate the capabilities of airborne LIDAR and hyperspectral remote sensing for the monitoring of beach morphodynamics.

Methodology

Table I summarizes the dates and sensors of the airborne hyperspectral and LIDAR acquisitions. Due to organizational constraints no recordings could be performed in 2003 and the LIDAR and hyperspectral acquisitions could not always be synchronized in time. In 2000 and 2001 both acquisitions were performed within one month, but in 2002 and in 2004 more time elapsed between the LIDAR and hyperspectral recordings. In 2000, 2001 and 2002 a hyperspectral CASI scanner was used. This instrument, developed by ITRES, measures the reflected sunlight in a 545 nm spectral range configured in the visual and near-infrared (VNIR) range. The 96 spectral bands were radiometrically calibrated, atmospherically corrected (Berk *et al.*, 1989; Richter and Schläpfer, 2002) and geometrically corrected.

Table I. Sensors and dates of the airborne hyperspectral and LIDAR acquisitions in the period 2000–2004

	2000	2001	2002	2004
Hyperspectral	CASI 23/08/2000	CASI 27/08/2001	CASI 11/10/2002	AISA-Eagle 6/07/2004
LiDAR	ALTM 1225 11/09/2000	ALTM 1225 28/09/2001	ALTM 1225 18/12/2002	ALTM 2050 2/09/2004

DOI: 10.1002/esp

Table II. Sediment parameters for each of the seven sand type classes used in the classification of the beach; based on the field sampling of 2004 (w% = weight percentage, c% = a percentage obtained after counting a sub-sample of 500 grains)

	D_{50} (mm)	Sorting (phi)	Carbonates (w%)	Organic matter (w%)	Fe (w%)	Shell fragments (c%)
Muddy sand/pure mud	<63	n/a	52.05	7.3	2.2	0
Fine sand of the lower shoreface	189	0.37	11.51	0.07	0.42	2.82
Fine–medium sand of the lower shoreface	239	0.39	10.54	0.02	0.41	4.53
Original sand of the upper shoreface	244	0.43	10.22	0.08	0.43	4.56
Sand used for beach nourishments	300	0.57	20.43	0.06	0.62	5.31
Shell-rich sand	381	0.84	42.97	0.1	0.85	7.68
Fine dune sand	217	0.34	7.14	0	0.4	2.85

In 2004, an AISA-Eagle was used. This sensor, developed by Specim, covers the VNIR range between 400 and 900 nm and was configured to capture the reflected light in 32 spectral bands. The smaller number of bands proved to be sufficient to classify the sand with high accuracy. This is due to the featureless nature of the spectra causing a high inter-correlation between adjacent bands. The spatial resolution (i.e. the pixel size) of all hyperspectral data was resampled to 2 m × 2 m, using nearest-neighbour resampling.

The hyperspectral data were used to classify the beach into seven sand type classes; these sediment facies classes were defined in the field to correspond to the most common sand types found along the Belgian coast and are linked to the topography and geomorphology of the beach; i.e., certain topographical or geomorphological units of the beach can be characterized by a certain type of sand. Table II lists the seven classes; the samples used to derive the parameters in this table are the ground truth samples that served as training and validation of the classifications of the AISA data of 2004. Note that these samples correspond to the upper millimetres of the sediment, as the reflectance is only determined by this top layer. Each airborne hyperspectral campaign was accompanied by a field sampling campaign that served to collect field samples to train and validate the classifications. An important element during the field sampling was the collection of both dry and wet samples for those classes that occur on both the intertidal and the supratidal beach. As the wetness of the sand has an influence on the spectral reflectance (the reflectance lowers in a quasi-homothetic way, i.e. without changing the shape of the spectrum, when the water content increases), it is important to take this variance into account when collecting the samples. The classification results pointed out that it is possible to group samples with a different water content in one class if the samples cover the entire variance present in the population of that particular class.

The hyperspectral data were classified with a linear discriminant classifier (LDC) (Fisher, 1936; Duda *et al.*, 2001) in combination with feature or band selection based on a sequential floating forward search algorithm (SFFS) (Pudil *et al.*, 1994). Briefly described, LDC performs as follows: for C classes and N bands, LDC projects the N-dimensional input vector onto a $(C - 1)$-dimensional vector with optimal class discrimination in mind. It minimizes the ratio of the within class over the between class scatter matrices. Hence, for a two-class problem, the feature space is projected onto a one-dimensional space, and the LDC technique immediately serves as a linear classifier. For this study, in which seven classes were to be distinguished, a multiple-binary approach was adopted. This means that the outputs of several binary classifications were combined to come to a final class decision. Kempeneers *et al.* (2005b) compared the multiple-binary classification approach with the more common multiclass approach and concluded that the multiple-binary approach outperforms the multiclass approach. The best classification results were obtained when the original spectral bands were transformed to wavelets (discrete Haar type wavelets). Using three wavelet coefficients, selected with SFFS, in each binary classification, resulted in an overall accuracy of 82% for the imagery of 2004. More information on the classification methodology used and the accuracy obtained can be found in the work of Deronde *et al.* (2006b) and Kempeneers *et al.* (2005a).

To reduce the number of data (i.e. bands) to be used in the classification algorithm and to take into account the limited number of training samples, which from a statistical point of view limits the number of bands that can be used (Kalayeh *et al.*, 1983), a feature selection step was necessary. A straightforward method would be to try all possible band combinations. This will always yield the best subset of features, but it is a very exhaustive and time-consuming approach. Therefore, the sequential floating forward search (SFFS) was used. SFFS performs as follows: one selects the best single band, then adds a second band to have the best combination of two bands, adds a third band to have the best combination of three bands and so on. However, after each forward step, SFFS performs one or more backward steps, i.e. it removes a previously selected feature to investigate whether the score can be increased using another

DOI: 10.1002/esp

band. This floating aspect was used to minimize the possibility of ending up in a local minimum. After the feature selection procedure a combination of N bands that are (sub)optimal for classification is obtained.

The LIDAR data served to create maps indicating the erosion and accretion. These maps could easily be obtained by subtracting the successive DTMs from each other. The DTMs were obtained after morphological filtering of the DEMs, i.e. all elements that do not belong to the Earth's surface, e.g. beach cabins, were eliminated. After filtering, the point density was reduced to one point every 16 m^2. The vertical accuracy of the DTMs on flat reference surfaces, expressed as the mean signed error (Su and Bork, 2006), was approximately 5 cm, with a standard deviation of 7 cm. The errors on the gentle sloping beach are not exactly known, as there were no reference surfaces, but according to the investigations of Su and Bork (2006) the mean signed error will not significantly increase for slopes between 0 and 15%. The volume differences were calculated in two ways: per polygon, where the polygons delineate areas with major volume changes between two dates; and per coastal zone, where zones are larger areas of a few kilometres long that integrate the beach between the low-water mark and the dune foot.

The final analysis (see the results section) is based on the combination of the DTMs, the erosion/accretion maps resulting from the subtracted DTMs and the classified hyperspectral images. The latter is the innovative aspect in this research. While DTMs only allow for a calculation of the amount of sediment eroded or deposited, the classified scenes allow for a qualitative interpretation in which the classes serve as tracer for the sediment dynamics. This is the fundamental reason why the hyperspectral images have to be classified into a number of sand type classes. Without these classes, it is not possible to derive any information on the direction of the sediment transport, as the raw hyperspectral data only offer a per pixel reflectance spectrum. In order to use these reflectance data for sand dynamics studies, one has to classify the hyperspectral data into classes that can be distinguished spectrally and that are related (however not inextricably) to certain geomorphological units of the beach. E.g. the class 'Fine sand of the lower shoreface' is typically found on the lower shoreface; it features a mineralogical composition, a grain size and a sorting that are the result of the processes acting on the lower shoreface; but it is possible that this class is found elsewhere on the beach. Hence, the classified images reveal information on the nature and the geomorphology of the beach. By studying the spatial dynamics of the classes, one gains knowledge of the morphodynamics of the beach.

Results

Before focusing on the three case studies, it is worthwhile to have a look at the volumetric changes over the entire beach. Table III summarizes these volumetric changes, the mean height difference and the total volume of nourished sand for the whole area considered. The latter was divided into five units, which are bordered by harbour channels or

Table III. Mean height difference, volume difference and total volume of nourished sand for the entire Belgian coastline, divided into five units and with a distinction between the foreshore and the backshore + foredunes. The time window is 2000–2004

	Time window	Foreshore mean height difference (cm)	Foreshore volume difference (m^3)	Backshore and foredunes mean height difference (cm)	Backshore and foredunes volume difference (m^3)	Nourished sand volume (m^3)
1. French border to channel of Nieuwpoort (14.3 km)	2001 – 2000	2.9	119 300	–2.8	–34 400	19 000
	2002 – 2000	6.7	273 200	11.6	143 600	38 000
	2004 – 2000	7.5	301 600	20.1	248 100	76 000
2. Channel of Nieuwpoort to the harbour of Oostende (16.6 km)	2001 – 2000	0.4	13 900	16.5	66 100	70 000
	2002 – 2000	1.5	49 809	26.7	107 200	140 000
	2004 – 2000	13.3	454 200	34.1	124 500	998 000
3. Harbour of Oostende to the harbour of Blankenberge (15.5 km)	2001 – 2000	0.7	23 400	11.2	81 400	21 000
	2002 – 2000	–6.6	–207 900	24.6	178 900	42 000
	2004 – 2000	–10.1	–312 800	32.9	236 600	84 000
4. Harbour of Blankenberge to the harbour of Zeebrugge (5.3 km)	2001 – 2000	0.3	4 800	5.5	18 500	0
	2002 – 2000	5	80 800	13.4	45 200	0
	2004 – 2000	13.5	207 500	17.2	57 800	0
5. Harbour of Zeebrugge to the Dutch border (10.1 km)	2001 – 2000	–7.8	–164 700	–2.2	–17 300	0
	2002 – 2000	–16.6	–351 700	1.4	10 700	0
	2004 – 2000	–0.4	–8 300	9.7	75 200	403 000

DOI: 10.1002/esp

dams. The reason to divide the coastline in this way is that the channels and harbour dams act as a barrier for the longshore transport. Hence, these units can be considered as entities without (or with a limited) input from the neighbouring units. This facilitates the analysis and interpretation.

The first and westernmost unit is characterized by minor nourishment activities in the form of beach berm replenishment works. The total volume difference on the beach largely exceeded the nourished volume, indicating that this is an accretional beach, bordered by dunes, which also grew in the period 2000–2004.

In the second unit, moderate volumes were deposited by means of berm replenishment works between 2000 and the beginning of 2004. In April–June 2004 an important beach nourishment took place in the centre of Oostende, resulting in a net volume difference for this unit of approximately +450 000 m^3 (foreshore) and +125 000 m^3 (backshore and foredunes) between 2000 and 2004. The 'emergency' nourishment in Oostende served to increase the safety level in the centre of Oostende; before the nourishment there was no longer a dry beach at high tide. The sea dike was the only protection to the city.

The third unit features a net loss of sand in the studied time frame: approximately 312 000 m^3 of sand eroded over 4 years, despite a total nourished volume of 84 000 m^3. However, it should be noted that before the period studied large-scale beach nourishments were executed: 3 200 000 m^3 in 1992–1996 and 260 000 in 1998–2000. The erosion in the following years can be interpreted as an adjustment of the beach towards a more natural profile. The sea-bordering dunes grew at the same rate as in the first two units.

The fourth unit is rather small, but it is a unique unit due to the location on the western side of the harbour dams of Zeebrugge. These dams are more than 4 km long and act as a perfect sand trap (the net longshore sediment transport is from the West to the East), causing the wide accretional beach in Zeebrugge (see the case study 'The Middle Coast in Zeebrugge'). The net volume difference (on foreshore, backshore and foredunes) was +265 000 m^3 without any nourishment carried out in the time lapse considered. Earlier, in 1998–1999, the backshore immediately West of Zeebrugge (at the Duinse Polders) was nourished with 490 000 m^3.

The last and most eastward unit is situated between the eastern harbour dam and the Dutch border. Despite some berm replenishment works and a maintenance beach nourishment in 2004, the net volume difference of the foreshore was negative (–8300 m^3). The sea-bordering dunes grew, but less fast than in the other four units. This unit will also be elaborated in the case studies.

Case Study: The West Coast in Koksijde

Figure 4 gives an overview of all thematic GIS layers used to analyse the coastal dynamics in a certain area. Note that the sand transport map (C) is an analysis product of the five base layers. The first striking pattern when looking at the height difference maps in Figure 4 is the parallel erosion and accretion areas on the intertidal beach (N° 1). These are caused by the cross-shore displacement of the ridges and runnels, characteristic of these wide dissipative beaches. The net resulting transport over a larger coastal section is close to zero. Note however that these images are snapshots taken at one moment in the year; the location of the ridges and runnels changes continuously, but these intra-year changes are not visible in our yearly observations. In Figure 4(B) one can see that fine to medium sand is dominant on this intertidal beach. Unfortunately, the hyperspectral acquisition of 2004 was performed close to high tide, leaving only the supratidal beach dry (in the last section of this paper we come back to the operational limitations of this technique). However, the small strip observed in 2004 (Figure 4(B)(2)) illustrates the accretion caused by the two groins at N° 2. In 1987–1988 both groins were constructed to counter the erosion that was taking place before. The area between and eastward of (N° 3) these groins is now accretional, and grew by 70 600 m^3 on the intertidal beach and 60 000 m^3 on the supratidal beach. Looking at the sand class map of 2000 (Figure 4(B)(1)), one can see that there is coarse and shell-rich sea sand on the dry beach (N° 4) caused by berm replenishment works (in the four years studied, 48 000 m^3 was deposited). Hence, the growth of the supratidal beach (N° 2) is a combination of man-made growth and natural accretion caused by the extended groins. The sand class map also suggests longitudinal transport of (fractions of) the nourished sand in the eastern direction (N° 5). However, one should be careful with this interpretation; the shell-rich sand found around N° 5 could also be the result of the lowering of the beach that occurred after the construction of the groins. The latter caused a starvation of the supply of sand from the west. This lowering could have been responsible for the formation of a deflation floor on which the rough and coarse sediment fractions were concentrated. Hence, the type of sand in this area may be the result of both an erosion process and an eastward longitudinal transport of nourished sand. The shell-rich sand found at N° 6 is caused by a local nourishment with sea sand. A last remarkable feature on this beach is the heavy erosion of the foredunes at N° 7. Shortly after the construction of the groins in Koksijde, the intertidal beach in front of the dunes lowered (see above). The lowering of the intertidal beach caused the dunes to be more exposed to storm surges. The erosion is clearly visible at N° 7.

DOI: 10.1002/esp

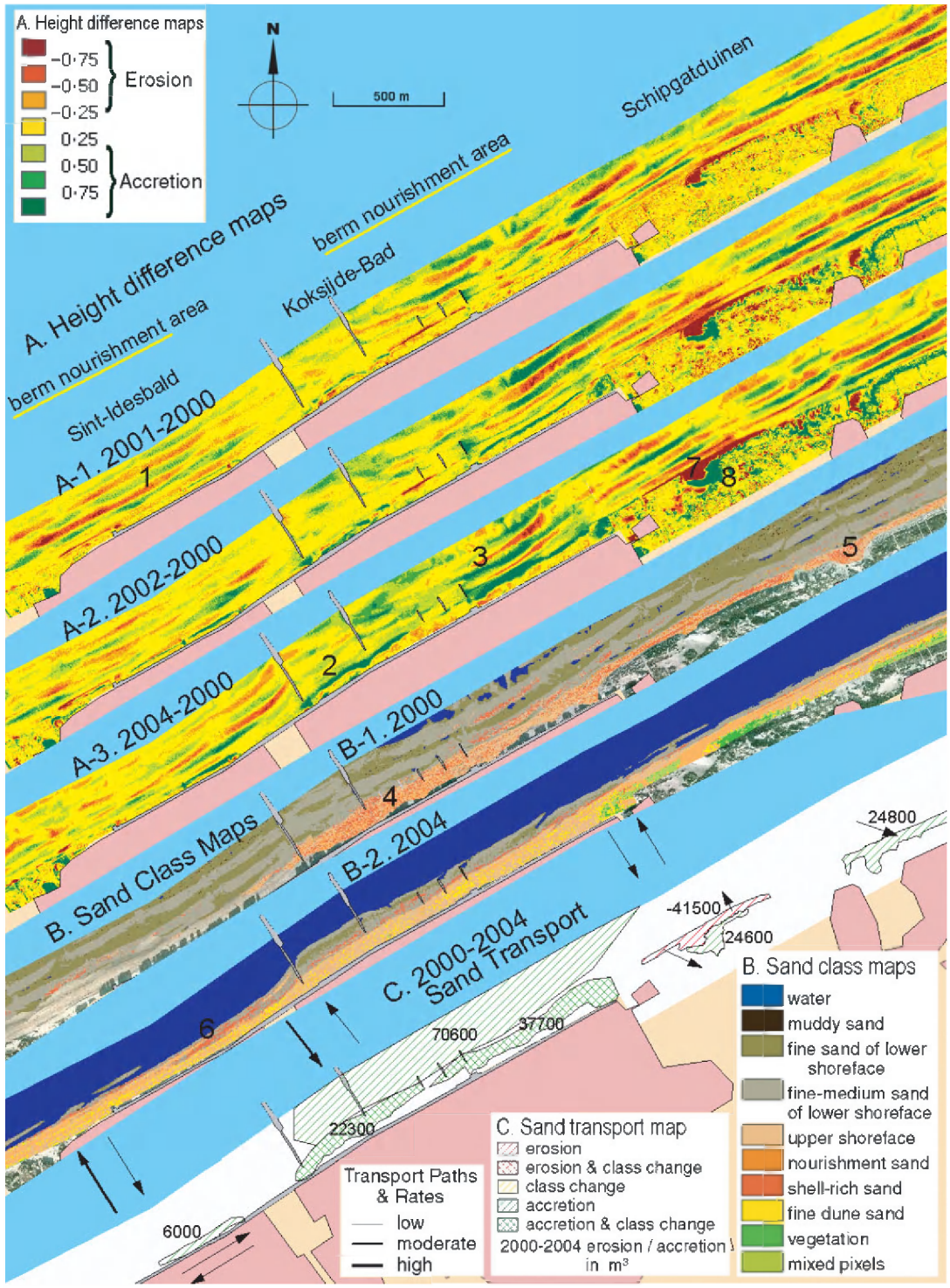

Figure 4. Different GIS layers used to analyse the sediment transport around the seaside resort of Koksijde. In top-down order, one can see the three height difference maps with the year 2000 as reference year, then two classified hyperspectral scenes featuring the sand classes in 2000 and 2004. At the bottom, the resulting sand transport for the period 2000–2004 is given; the arrows indicate the direction and amount of sand transport.

DOI: 10.1002/esp

Locally aeolian deflation adds to the dunefront erosion. The aeolian transport is directed landwards and deposition takes place on the lee-side of the eroded dune (N° 8). More recent surveys seem to indicate the intertidal beach around the groins is attaining a new equilibrium state, allowing more transport eastward. This will most probably stop the lowering of the intertidal beach in front of N° 8 and the landward retreat of the foredunes.

Case study: The Middle Coast in Zeebrugge

The most striking pattern in this coastal strip is the large accretional beach on the western side of the harbour dam of Zeebrugge (Figure 5, N° 1). The net West-to-East transport resulted in the deposition of approximately 336 000 m^3 in the four years studied. West of this deposition area, the beach nourishment area of the Duinse Polders stands out (N° 2). The backshore berm created in 1998–1999 is clearly distinguishable on the classified hyperspectral scenes due to the type of sand used: it is somewhat coarser grained and it contains more shells and iron than the sand naturally found on this part of the beach. The fill is eroded during high tide and storm events. The reason for the beach nourishment should be sought in the extension of three groins in Blankenberge in 1985–1986 and 1991. They act as a sand trap in the longshore transport, resulting in accretion between the groins. However, this beneficial effect led to a reduction in the supply of sand in the area of the Duinse Polders, and hence to a lowering of the foreshore and the backshore.

On the three height difference maps (Figure 5(A)) one can see clearly that the berm is gradually eroded year after year, causing a landward retreat of the seaward border of the nourished berm. Some of the nourishment sand is deposited on the lower parts of the beach (N° 3) and eastward along the high-water mark (N° 4). It contributes to the accretion area mentioned above, but the total volume eroded on the intertidal and supratidal beach (approximately 108 000 m^3 at the nourishment site; see Figure 5(C)) is much lower than the amount deposited eastward, indicating that the deposited volume mainly consisted of natural, non-nourished sand that is supplied through longshore transport processes. This assumption is confirmed by the classified maps, indicating that the deposited sand mainly consisted of fine and medium sand of the intertidal beach. The yellow class found on the highest parts of the beach and in the foredunes (N° 5) is a fine quartz fraction transported and deposited by aeolian processes. The source area of this sand is the nourished berm but also the non-nourished supratidal beach westwards. The small area indicated as nourishment sand at N° 6 is not natural; it is the remnant of a man-made sand castle, built with sand mixed with cement.

Case study: The East Coast in Knokke-Heist

The third case study concerns the beach in the centre of Knokke-Heist. As mentioned before, this unit has for many decades been prone to heavy erosion, causing it to be the first place along the Belgian coast where large-scale beach nourishments were executed (1978–1980; locally renourished in 1986, 1999 and 2004; see Figure 6, top). The effects of these interventions are clearly visible on the different layers in Figure 6: in Figure 6(B) one can see that the supratidal beach largely consisted of nourishment sand. The 1999 fill could spectrally be distinguished because it contains coarse-grained, poorly sorted sand containing a lot of shells, and even some gravel (N° 1). The reflectance is lower and the colour more reddish due to the iron-rich sand used (borrowed from banks offshore). The two first height difference maps (Figure 6(A)(1) and (2)) show clearly the erosion of the nourished berm at the seaward side (N° 2) as well as the erosion of the lower parts of the intertidal beach (N° 3). A few weeks before the airborne campaigns of 2004, a maintenance nourishment was executed (N° 4 and 5). Once again, the fill was quickly eroded and reworked, i.e. the shells were washed out and temporarily stocked on the intertidal beach (N° 6). This can be explained by the high wave energy in the swash zone, leading to the uptake of coarse sediments and shells in the uprushing water flow. During the backwash (i.e. the flow of water back to sea) there is no wave energy and the heavy shells are deposited (Short, 2001). The muddy sand along the low water level (N° 7) may correspond to a temporary veneer of mud deposited on the lower parts of the beach under quiet meteorological conditions (the offshore part of these beach sections is largely muddy). In the foredunes, the class with fine dune sand is widespread (N° 8); it is deposited between the vegetation and the artificial fences on the foredunes.

The figure illustrating the net sand transport (Figure 6(C)) is rather difficult to interpret due to the extra nourishment between the two last acquisitions. However, it can be concluded that, despite the recent nourishment, the intertidal and to a lesser extent also the supratidal beach were largely erosive. At N° 9, where the nourished volume was smaller and limited to a small strip (20 m wide), the net erosive character of the intertidal beach becomes clear, despite a net growth of the supratidal beach and the foredunes. The eroded sand is, after temporary stock of certain fractions on the intertidal beach, mainly transported nearshore, although longshore transport to the East also occurred. The latter is

DOI: 10.1002/esp

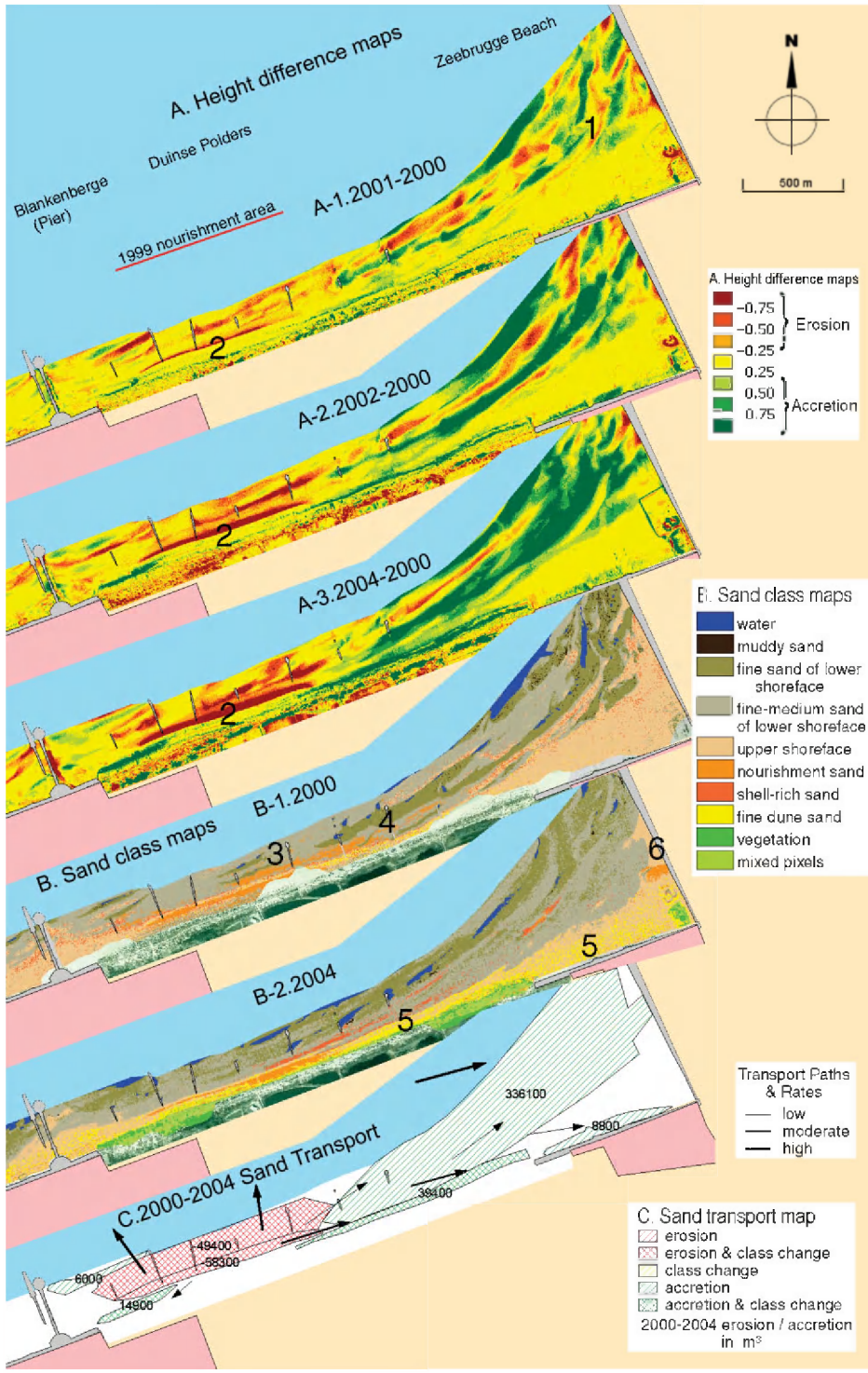

Figure 5. Different GIS layers used to analyse the sediment transport between the pier of Blankenberge and the harbour dam of Zeebrugge. In top-down order one can see the three height difference maps with the year 2000 as reference year, then two classified hyperspectral scenes featuring the sand classes in 2000 and 2004. At the bottom, the resulting sand transport for the period 2000–2004 is given; the arrows indicate the direction and amount of sand transport.

DOI: 10.1002/esp

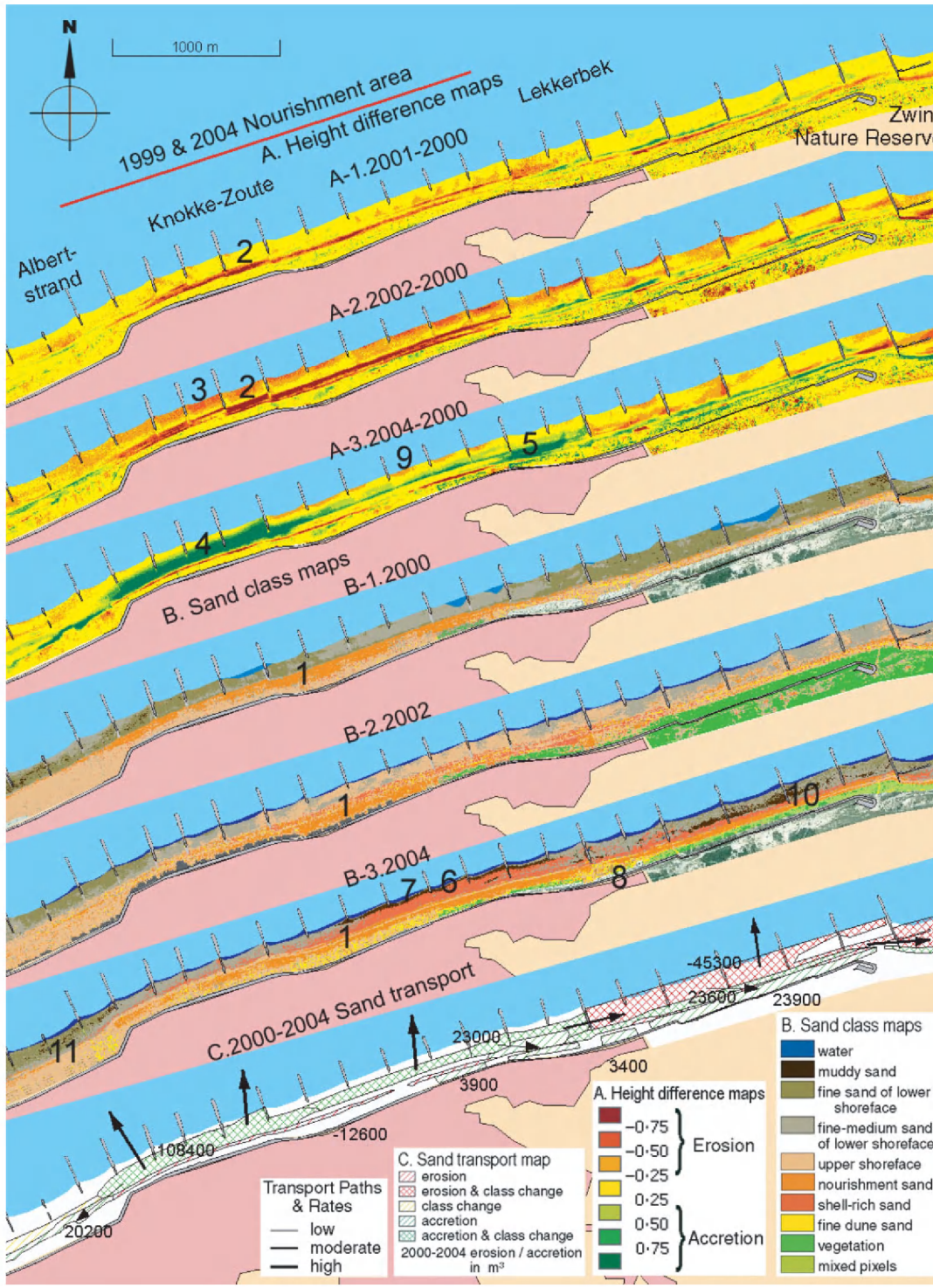

Figure 6. Different GIS layers used to analyse the sediment transport in the city of Knokke-Heist. In top-down order one can see the three height difference maps with the year 2000 as reference year, then three classified hyperspectral scenes featuring the sand classes in 2000, 2002 and 2004. At the bottom, the resulting sand transport for the period 2000–2004 is given; the arrows indicate the direction and amount of sand transport.

DOI: 10.1002/esp

confirmed by Figure 6(B)(3), where nourished sand was found all along the high-water mark eastwards of the nourished areas (N° 10); westwards almost no influence of the nourishment could be observed (N° 11).

Discussion

The case studies presented above do not only demonstrate the capabilities of airborne hyperspectral remote sensing and LIDAR to map and monitor the transport of beach sediments, they also illustrate the response of a sandy beach to different protection measures. On the Belgian coast, three types of measure are currently in use: (beach) groin fields, beach nourishments and berm replenishments. In Koksijde, long groins were combined with berm replenishments and the area of the Duinse Polders was subject to a backshore and dune front nourishment, whereas in Knokke-Heist the shoreline is protected by a groin field. However, the latter did not keep the beach from eroding, and subsequently several large-scale beach nourishments, covering both the backshore and the foreshore, were carried out in Knokke-Heist. In the last two decades, preference has been given to soft defence structures such as beach nourishments and berm replenishments rather than hard structures such as groins. The main reason for this choice is that soft defence structures (i.e. adding sand to the system) have a smaller impact on the natural dynamics of the beach and provide a better barrier in case of heavy storms (Dean, 2002). Since dredging of harbour channels is a regular necessity, deposition of the dredged material on the beach (supplemented as needed by other deep water sources) has been seen by many as a win–win solution. However, though beach nourishments are generally considered as an environment-friendly and efficient option for coastal protection and beach restoration, it should be noted that this technique may have ecological impacts in both the short and the longer term (see Speybroeck *et al.*, 2006, for a review).

The second and third case studies showed varying degrees of beach nourishment efficiency. Clearly, the Duinse Polders backshore and dunefront nourishment has a larger retention period and it is inferred that the losses to the nearshore are probably intercepted at the nearby Zeebrugge harbour dam, which is located downdrift with respect to the Duinse Polders site. The retention period of the 1999 and 2004 nourishment in Knokke-Zoute is in comparison much shorter, about 5 years. Between the two nourishments, approximately 55% of the 1999 fill was transported longshore and appeared to add to the, mostly downdrift, backshore and dunefront area. This conclusion can be drawn with the help of the classified hyperspectral data, which indicate the presence of nourishment sand in this area. The option that this sand volume is still a remnant of the nourishments in 1978–1980 is not retained, as it was observed (e.g. at the Duinse Polders) that a nourishment fill is subject to re-sorting, especially on the foreshore; hence, the 20-year-old fill would no longer be classified as nourishment sand. The remainder of the losses were transported to the foreshore and further down to the nearshore, from where they were removed from the area, as the foreshore and the neighbouring nearshore also continue to erode.

As hard structures perpendicular to the coastline, groins act as a trap for the longshore transport and stimulate the sedimentation between them. The drawback of this measure is that they seriously impede dynamic beach behaviour and that by intercepting sand from the longshore transport they cause erosion downdrift. Hence, the beneficial effect between the groins is often accompanied by a negative side-effect a few kilometres further. The negative influence continues as long as a new equilibrium state between and around the new or extended groins is not attained. A good example of the theory above was observed in Koksijde-bad, where the beach in front of the Schipgatduinen lowered due to the construction of two groins in 1987–1988. The same process was the cause of the beach erosion at the Duinse Polders in the 1990s.

The main added value of the hyperspectral data is the ability to analyse the direction of the sediment transport. Although sediment volumes are subject to re-sorting processes, which sometimes hamper the analysis as this influences the classification results, the classified hyperspectral scenes offer insight in the directions of the sediment transport. LIDAR, or topographical data in general, offer only local height information.

Considerations Regarding Future Monitoring Strategies

Although hyperspectral remote sensing is a very powerful technique in itself, its added value is best manifested when combined with other remote sensing data, in this case laserscan data. Despite the obvious potential of data fusion techniques, this methodology is still novel. Most remote sensing based research is based on one single type of data. An important reason for this is the logistical and financial aspect. Both hyperspectral and LIDAR data are today only available from airborne platforms. The CHRIS instrument on board the PROBA satellite and the Hyperion sensor on EO-1 offer spaceborne hyperspectral data, but the radiometric quality and the spatial resolution is much lower than the specifications we are used to when working with airborne data. Moreover, their fixed orbit is not compatible with

DOI: 10.1002/esp

observations bounded by meteorological and tidal constraints. Therefore, expensive airborne acquisitions are the only option today. This is probably the main reason why the technique illustrated above is not widespread yet. Currently, new platforms and sensors are being built; by 2009–2010 a new generation of hyperspectral satellite sensors should become operational. They will have an increased radiometric performance, but will still be limited from an operational point of view. To overcome this, entirely new platforms are being developed: unmanned aerial vehicles (UAVs) cruising in the stratosphere for several weeks or even months will drastically reduce the cost of airborne campaigns without losing the operational flexibility characteristic of airborne surveys (for more information see http://www.pegasus4europe.com). It is expected that these new platforms, which in a later stage will also be designed to carry active systems such as laserscanners, will announce a new era of coastal surveying, allowing an almost continuous and cost-effective monitoring strategy. The latter will allow us to study the sediment dynamics on a much smaller timescale, revealing more insight into the transport processes. Today, the yearly observations only allow for a longer-term analysis. The first operational UAV systems are to be expected in 2008.

Conclusions

Airborne hyperspectral data were classified into seven sand type classes following a multiple-binary classification approach based on sequential floating forward search and linear discriminant analysis, while LIDAR data were morphologically filtered to obtain DTMs with a vertical accuracy (mean signed error) of 5 cm. Subtracting sequential DTMs resulted in height difference maps indicating the erosion and accretion zones. The combined interpretation of both data types allowed analysis of the sediment dynamics along the Belgian shoreline. The technique was demonstrated at three sites. Koksijde, located on the West Coast and characterized by wide accretional beaches, is bordered in the Southeast by a high active dune barrier. Much of the accretion was triggered by the extension of two groins and was supplemented by berm replenishment works. In Zeebrugge, on the Middle Coast, a beach nourishment was executed one year before the data acquisition started. The hyperspectral data allowed to distinguish the nourished berm and to detect how the fill was eroded and how the nourished sand was redistributed. East of the nourished area, the dam of the harbour of Zeebrugge halts the longshore transport, causing a wide accretional beach. The third site, Knokke-Heist, is situated on the East Coast and is characterized by narrow and rather steep beaches, heavily influenced by nourishment activities. The three sites allowed demonstration of the potential of the joint use of airborne hyperspectral data and LIDAR data. While LIDAR data only offer topographical information, hyperspectral data, and especially the combination of the two, allow for an analysis of the sediment transport directions. Despite the huge potential of the techniques demonstrated, the high cost of the data acquisition is today a major drawback. New unmanned platforms will hopefully reduce the cost of this type of acquisition, heralding a new era in remote sensing based coastal studies.

Acknowledgement

The authors are very grateful to the Flemish Government – Agency for Maritime and Coastal Services – Coastal Division, who gave us the possibility to explore these innovative remote sensing techniques. We in particular thank Ir. Peter De Wolf and Ir. Kevin Delecluyse for their interest and support.

References

Baeteman C, Declercq PY. 2002. A synthesis of early and middle holocene coastal changes in the Western Belgian lowlands. *Belgisch Tijdschrift voor Geografie* **2**: 7–107.

Beets DJ, van der Spek AJF. 2000. The Holocene evolution of the barrier and the back-barrier basins of Belgium and the Netherlands as a function of late Weichselian morphology, relative sea-level rise and sediment supply. *Geologie en Mijnbouw* **79**(1): 3–16.

Berk A, Bernstein LS, Robertson DC. 1989. *MODTRAN: A Moderate Resolution Model for LOWTRAN7*, Report GL-TR-890122. Air Force Geophysics Lab: Bedford, MA.

Bird ECF. 2000. *Coastal Geomorphology, an Introduction*. Wiley: Chichester.

Brock JC, Wright CW, Sallenger AH, Krabill WB, Swift RN. 2002. Basis and methods of NASA airborne topographic mapper LIDAR surveys for coastal studies. *Journal of Coastal Research* **18**(1): 1–13.

Cracknell AP. 1999. Remote sensing techniques in estuaries and coastal zones – an update. *International Journal of Remote Sensing* **19**(3): 485–496.

Dean RG. 2002. *Beach Nourishment: Theory and Practice*. World Scientific: River Edge, NJ.

De Moor G. 2006. *Het Vlaamse Strand, Geomorfologie en Dynamiek*. VLIZ: Oostende.

Deronde B, Houthuys R, Debruyn W, Fransaer D, Van Lancker V, Henriet JP. 2006a. Using airborne hyperspectral data and laserscan data to study beach morphodynamics along the Belgian coast. *Journal of Coastal Research* **22**(5): 1108–1118.

Deronde B, Kempeneers P, Forster RM, Debruyn W. 2006b. Imaging spectroscopy as a tool to study sediment characteristics on a tidal sand bank in the Westerschelde. *Estuarine Coastal and Shelf Science* **69**(3/4): 580–590.

De Wolf P, Houthuys R. 1997. Evaluation of a beach nourishment combined with a nearshore feeder berm realized at the Belgian coast. *Proceedings of the Coastal Zone 97 Conference*, Boston, MA, 1997.

Duda RO, Hart PE, Stork DG. 2001. *Pattern Classification*. Wiley: New York.

Fisher R. 1936. The use of multiple measures in taxonomic problems. *Annals of Eugenics* **7**: 179–188.

Goetz AFH. 1992. Principles of narrow band spectrometry in the visible and IR: instruments and data analysis. In *Imaging Spectroscopy: Fundamental and Prospective Applications*, Toselli F, Bodechtel J (eds). Kluwer: Dordrecht; 21–32.

Houthuys R, De Moor G, Somme J. 1993. The shaping of the French–Belgian North Sea Coast throughout recent geology and history. In *Coastlines of the Southern North Sea*, Hillen R, Verhagen J (eds). American Society of Civil Engineers: New York; 27–40.

IPCC. 2001. *Climate Change 2001: Synthesis Report*. IPCC: Geneva.

Kalayeh HM, Muasher MJ, Landgrebe DA. 1983. Feature selection with limited training samples. *IEEE Transactions on Geoscience and Remote Sensing* **21**(4): 434–438.

Kempeneers P, De Backer S, Debruyn W, Coppin P, Scheunders P. 2005a. Generic wavelet-based hyperspectral classification applied to vegetation stress detection. *IEEE Transactions on Geoscience and Remote Sensing* **43**: 610–614.

Kempeneers P, De Backer S, Provoost S, Debruyn W, Scheunders P. 2005b. Hyperspectral classification applied to the Belgian coastline. *Proceedings of the SPIE International Symposium on Remote Sensing* 144–152.

Malthus TJ, Mumby PJ. 2003. Remote sensing of the coastal zone: an overview and priorities for future research. *International Journal of Remote Sensing* **24**(13): 2805–2815.

McLachlan A, Jaramillo E, Donn TE, Wessels F. 1993. Sand beach macrofauna communities: a geographical comparison. *Journal of Coastal Research* **15**: 27–38.

Mills E. 2005. Insurers in a climate of change. *Science* **308**: 1040–1044.

Mumby PJ, Edwards AJ. 2002. Mapping marine environments with IKONOS imagery: enhanced spatial resolution can deliver greater thematic accuracy. *Remote Sensing of Environment* **82**: 248–257.

Pudil P, Novovièová J, Kittler J. 1994. Floating search methods in feature selection. *Pattern Recognition Letters* **15**(1): 1119–1125.

Revell DL, Komar PD, Sallenger AH. 2002. An application of LIDAR to analyses of El Niño erosion in the Netarts littoral cell, Oregon. *Journal of Coastal Research* **18**(4): 792–801.

Richter R, Schläpfer D. 2002. Geo-atmospheric processing of airborne imaging spectrometry data. Part 2: Atmospheric/topographic correction. *International Journal of Remote Sensing* **23**(13): 2631–2649.

Rottier H, Arnoldus H. 1984. *De Vlaamse kustvlakte van Calais tot Saeftinge*. Lannoo: Tielt.

Sallenger AH, Krabill WB, Swift RN, Arens J, List JH, Hansen M, Holman RA, Manizade S, Sontag J, Meredith A, Morgan K, Yunkel JK, Frederick EB, Stockdon H. 2003. Evaluation of airborne topographic LIDAR for quantifying beach changes. *Journal of Coastal Research* **19**(1): 125–133.

Short AD. 2001. *Handbook of Beach and Shoreface Morphodynamics*. Wiley: Brisbane.

Speybroeck J, Bonte D, Courtens W, Gheskiere T, Grootaert P, Maelfait JP, Mathys M, Provoost S, Sabbe K, Stienen EWM, Van Lancker V, Vincx M, Degraer S. 2006. Beach nourishment: an ecologically sound coastal defence alternative? A review. *Aquatic Conservation: Marine and Freshwater Ecosystems* **16**(4): 419–435.

Stockdon HF, Sallenger AH, List JH, Holman RA. 2002. Estimation of shoreline position and change using airborne topographic LIDAR data. *Journal of Coastal Research* **18**(2): 502–513.

Su J, Bork E. 2006. Influence of vegetation, slope, and LIDAR sampling angle on DEM accuracy. *Photogrammetric Engineering and Remote Sensing* **72**(11): 1265–1274.

van der Wal D. 1998. The impact of the grain-size distribution of nourishment sand on aeolian sand transport. *Journal of Coastal Research* **14**(2): 620–631.

van der Wal D. 2000a. Grain-size-selective aeolian sand transport on a nourished beach. *Journal of Coastal Research* **16**(3): 896–908.

van der Wal D. 2000b. Modelling aeolian sand transport and morphological development in two beach nourishment areas. *Earth Surface Processes and Landforms* **25**: 77–92.

White SA, Wang Y. 2003. Utilizing DEMs derived from LIDAR data to analyze morphologic change in the North Carolina coastline. *Remote Sensing of Environment* **85**: 39–47.

Wright LD, Thom BG. 1977. Coastal depositional landforms, a morphodynamic approach. *Progress in Physical Geography* **1**: 412–459.